

# Multi-Class Wheat Moisture Detection with 5GHz Wi-Fi: A Deep LSTM Approach

<sup>†</sup>Weidong Yang, <sup>‡</sup>Xuyu Wang, <sup>†</sup>Shui Cao, <sup>†</sup>Hui Wang, and <sup>‡</sup>Shiwen Mao

<sup>†</sup>College of Information Science and Engineering, Henan University of Technology, Zhengzhou, Henan, P.R. China 450066

<sup>‡</sup>Department of Electrical and Computer Engineering, Auburn University, Auburn, AL 36849-5201 USA

Email: Yangweidong@haut.edu.cn, xzw0029@tigermail.auburn.edu, iscshuai@163.com, detehkn@gmail.com, smao@ieee.org

**Abstract**—Moisture content of cereal grains is a highly important factor in safe storage and food processing. The existing detection methods are either time-consuming, sensitive to the environment, or have a high cost. In this paper, we propose DeepWMD, a deep LSTM network based system for multi-class wheat moisture detection. We first collect CSI amplitude and phase difference data to detect wheat moisture content. Then, we design the DeepWMD system with commodity Wi-Fi devices in the 5GHz band, including data preprocessing of collected CSI data, offline training, and online testing. Our experimental results verify the efficacy of the proposed DeepWMD system, and demonstrates that DeepWMD can achieve high-precision multi-class wheat moisture detection in different indoor storage environments.

**Index Terms**—Channel state information (CSI); commodity Wi-Fi; phase difference; wheat moisture detection; deep learning; long short-term memory (LSTM).

## I. INTRODUCTION

With the growth of the world population and the improvement of people's life quality, the demands on the quality and quantity of cereal grains become more stringent, and are increasing rapidly every year [1]–[5]. In fact, more than two billion tons of grain are harvested annually [6]. How to store safely the harvested grains for meeting the future grain demand becomes highly important, especially for emergency demand scenarios such as famine or natural disasters [7]. Two physical factors, including moisture content and temperature, greatly influence the safe storage of grains [6]. Compared with the temperature factor, moisture content of cereal grains is more important in different phases of the grain distribution chain between the producer and consumer, which is one of the most important factors that determine quality. It is also an important factor in determining the proper time for harvesting, and has great influence on safe storage and selling price.

The existing grain moisture content measurement techniques include destructive methods [8] and non-destructive methods [9]–[14]. The destructive methods, such as oven-drying [8], are usually time-consuming, which requires oven-drying for specific time periods at a specific temperature. Thus, the destructive methods are not proper for widely deployment in the grain trade. On the other hand, non-destructive methods use the electric properties or the magnetic field to determine the grain moisture content, which require less man power and

are less time-consuming. However, the exiting non-destructive methods still have some limitations. For example, the capacitive method has the shortcoming that the measured grain moisture values are sensitive to the environment temperature and the grain flow velocity in the dryer [9]. Moreover, although the resistance method [10], the microwave method [11], [12], and the neutron method [13] can obtain high accuracy and achieve fast detection, the detection devices for these non-destructive methods entail a high cost.

In this paper, we propose to use Wi-Fi Channel state information (CSI) for non-destructive grain moisture content measurement. The CSI represents fine-grained channel information, thus reflecting the indoor channel features such as shadowing fading, multipath effect, and distortion [15]. Moreover, CSI amplitude data [16], [17] and phase difference data [18] have been shown to be highly stable, compared with received signal strength (RSS). By modifying the open-source device driver for off-the-shelf Wi-Fi network interface cards (NIC), we can read CSI values for received Wi-Fi packets from all the three antennas of the IEEE 802.11n NIC. For example, using Intel Wi-Fi Link 5300 NIC [15] and Atheros 9380 NIC [19], we can extract 90 CSI values and 168 CSI values for each received packet from the three antennas for the 20 MHz Wi-Fi channel, respectively, while the NIC can operate either in 2.4 GHz or 5 GHz. Moreover, the stable phase difference data in 5 GHz can be obtain when the transmitter and the receiver are equipped with the Intel Wi-Fi Link 5300 NIC, and are set in the inject model and monitoring model, respectively [18].

Recently, CSI data has been employed for indoor localization and device-free sensing. For indoor localization, DeepFi [16], [17] and FIFS [20] systems are based on CSI amplitude values for fingerprinting based localization; the PhaseFi [21], [22] and the BiLoc system [18] employ calibrated CSI phase data and bimodal CSI data as fingerprints for indoor localization, respectively, using a deep autoencoder network. To improve localization accuracy and reduce data storage, the CiFi system [23] and ResLoc system [24] leverage CSI images and tensor for indoor localization, using a deep convolution network and deep residual sharing learning, respectively. On the other hand, CSI data has been

used for device-free sensing, including fall detection, activity recognition, and breathing and heart rates monitoring. For fall detection, RT-Fall [25] and WiFall [26] consider CSI phase differences and amplitude to detect the fall of a patient, respectively. For activity recognition, E-eyes system [27] and The CARM system [28] can effectively recognize the different activity in indoor environments. For breathing and heart rate monitoring, PhaseBeat [29] and TensorBeat [30] exploit CSI phase difference data to monitor a single or multiple persons' breathing rates. Motivated by the existing CSI-based sensing techniques, our previous work has used CSI amplitude and phase difference data for wheat moisture detection, which is a binary classification method for detection of anomaly wheat moisture content [31].

In this paper, we focus on the multi-class wheat moisture content detection using CSI amplitude and phase difference data using 5GHz Wi-Fi, which is different from the anomaly detection of wheat moisture with support vector machine (SVM) based binary classification method [31]. In our experiments, we collect CSI amplitude and phase difference data on five different levels of wheat moisture content, ranging from 10.6% to 14.9%, in order to achieve multi-class wheat moisture content detection. We find that although most of the wheat moisture content levels have different CSI amplitude or phase difference values, there are still highly similar CSI values for different wheat moisture content levels, which brings a challenge for multi-class wheat moisture detection using traditional machine learning methods such as SVM. Thus, we exploit the deep long short-term memory (LSTM) method to handle the above similar CSI values for achieving a higher detection accuracy. In fact, the deep LSTM network has a stronger data representation capability than traditional machine learning methods [32], [33], which has been successfully applied for speech recognition [34], human activity recognition [35], and indoor localization [36].

In particular, we design DeepWMD, a **Deep** LSTM network based multi-class **Wheat Moisture Content Detection** system. The proposed DeepWMD system includes a data preprocessing module to collect CSI amplitude or phase difference data, and then normalize the amplitudes or phase differences of CSI data. The DeepWMD system has an offline training phase, where a two-layer deep LSTM network and a softmax classifier are trained with collected data. The deep LSTM network can achieve a stronger learning and representation ability. Moreover, the softmax classifier uses the cross-entropy to measure the difference between true labeled data and the normalized output data, and employs L2 regularization to avoid over-fitting. The back propagation through time (BPTT) algorithm is incorporated for training the deep LSTM network. For the online phase, an improved predication method is developed for determining wheat moisture content level with newly received CSI amplitude or phase difference data.

The main contributions of this paper are summarized as follows:

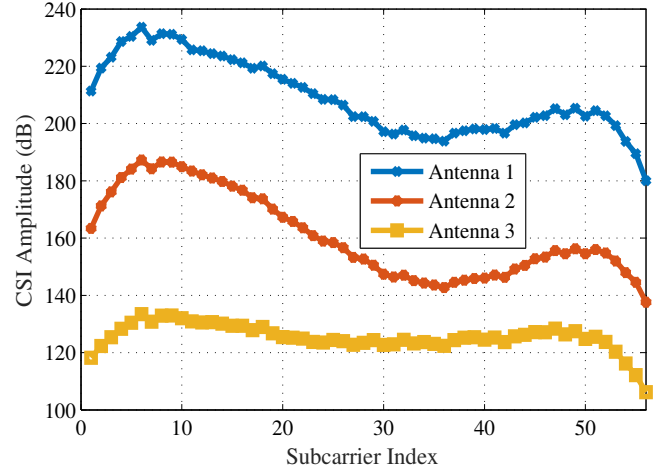


Fig. 1. CSI amplitude measurements for different antennas over subcarriers in LOS environment.

- We validate the feasibility of using fine-grained CSI amplitude and phase difference data for multi-class wheat moisture detection. To the best of our knowledge, this is the first work that leverages a deep LSTM network to detect multi-class wheat moisture.
- We design the DeepWMD system, which collects CSI amplitude and phase difference data to train the deep LSTM network, respectively, and then employ newly received CSI data for determining the moisture content of cereal wheat. The DeepWMD system includes data preprocessing, offline training, and online testing modules.
- We also implement DeepWMD on two off-the-shelf laptop computers with commodity Wi-Fi cards. The experiment results demonstrate that the proposed DeepWMD system can achieve considerably high classification accuracy in both line-of-sight (LOS) and non-line-of-sight (NLOS) scenarios.

The remainder of this paper is organized as follows. The preliminaries are discussed in Section II. We present the DeepWMD system design in Section III and evaluate its performance in Section IV. Section V concludes this paper.

## II. PRELIMINARIES AND FEASIBILITY

### A. Channel State Information

Modern wireless communication systems such Wi-Fi and LTE mainly adopt OFDM techniques in the Physical Layer (PHY) [37]. The OFDM technique can separate the total spectrum into multiple orthogonal subcarriers, where data can be sent over subcarriers for addressing the frequency selection fading in complex indoor scenarios [38]. For the OFDM technique in Wi-Fi system, the subcarriers can be considered as narrowband flat fading channels. We define  $H_i$  as the CSI value of the  $i$ th subcarrier, that is

$$H_i = |H_i| \exp \{j\angle H_i\}, \quad (1)$$

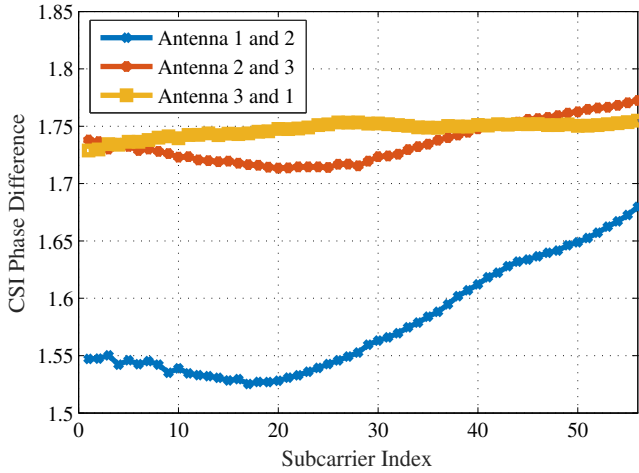


Fig. 2. CSI phase difference measurements for different antenna pairs over subcarriers in LOS environment.

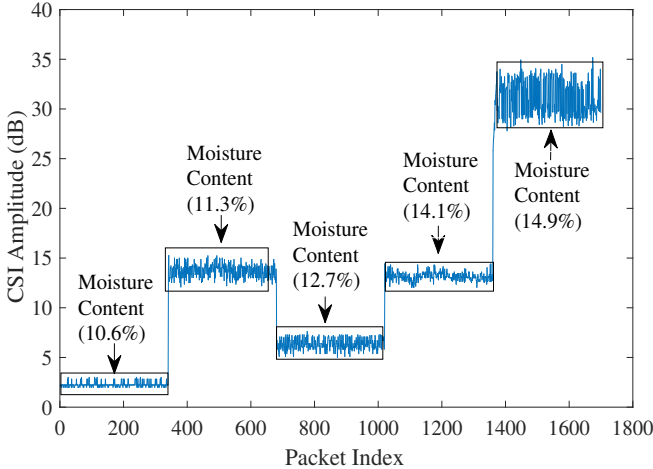


Fig. 3. CSI amplitude measurements for five different wheat moisture contents.

where  $|H_i|$  and  $\angle H_i$  are the amplitude and phase information for the  $i$ th subcarrier, respectively.

Recently, CSI data has been leveraged for RF sensing such as fall detection, activity recognition, breathing and heart rate monitoring, and indoor localization [16], [29], [39]–[41], because CSI data can offer fine-grained channel information, reflecting indoor channel characteristics such as distortion, multipath effect, and shadowing fading. For example, Fig. 1 and Fig. 2 show CSI amplitude and phase difference measurements over subcarriers in the LOS environment using the Atheros 9380 NIC, respectively. We can see that the CSI values are highly different for different antennas over subcarriers, which can be used for multi-class wheat moisture detection using the deep LSTM network.

#### B. Our Experiment Observation

We first experimentally verify the feasibility of using CSI amplitude and phase difference data for wheat moisture de-

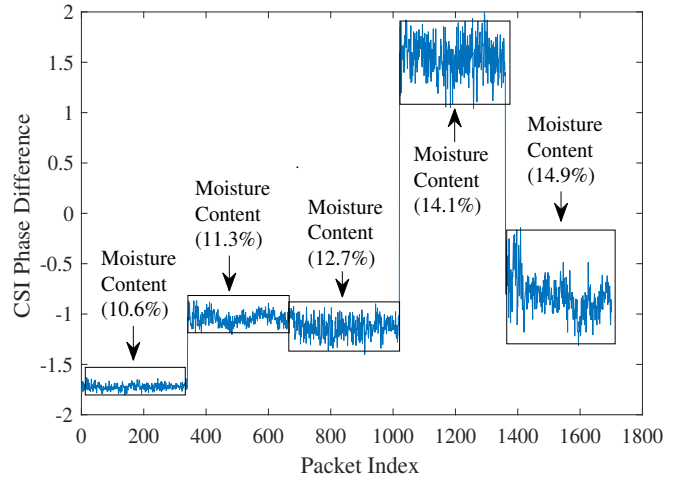


Fig. 4. CSI phase difference measurements for five different wheat moisture contents.

tection, using the binary classification SVM based method proposed in our prior work [31] for anomaly detection of wheat moisture content. In this experiment, we collect CSI amplitude and phase difference data that pass through wheat over five moisture content levels, ranging from 10.6% to 14.9%. Fig. 3 shows the CSI amplitude measurements for five different wheat moisture content levels. It is noticed that for most of the wheat moisture content levels, the corresponding CSI amplitude values are different. However, when the wheat moisture contents are 11.3% and 14.1%, the CSI amplitude values are close to each other, which leads to a big challenge for distinguishing these two content levels.

Fig. 4 shows the CSI phase difference measurements for five different wheat moisture content levels. As we can see, different wheat moisture content levels has also different CSI phase difference values. Only for wheat moisture content levels at 11.3% and 12.7%, the CSI phase difference values are close to each other. To deal with such cases, we propose to leverage a deep LSTM network to achieve a higher multi-class wheat moisture detection accuracy. This is because the deep LSTM network has a stronger data representation capability than traditional machine learning methods such as SVM.

### III. THE DEEPWMD SYSTEM DESIGN

#### A. DeepWMD System Architecture

The DeepWMD system consists of two Wi-Fi devices, while one is set as the transmitter and the other as the receiver. Both of them are equipped with an Intel Wi-Fi link 5300 NIC. Moreover, to obtain 5 GHz CSI amplitude and phase difference data, the transmitter and receiver are configured in the *injection mode* and the *monitoring mode*, respectively.

Fig. 5 shows the proposed DeepWMD system, including data preprocessing, offline training, and online testing components. First, the DeepWMD system calibrates the collected wheat moisture data to obtain a clear CSI data sequence. Then,

for offline training, the DeepWMD system employs use captured data from five different moisture content levels to train a deep LSTM network, while a softmax classifier is used in the top layer for classification. The LSTM model can effectively handle sequence based data, and also has a strong classification capability for multi-class wheat moisture detection. For online testing, the newly collected CSI data is fed into the well-trained LSTM model to detect the closest wheat moisture level among five known, different wheat moisture content levels.

### B. Data Preprocessing

We measure CSI data from five wheat piles with different moisture content levels. In this experiment, we transmit 1000 packets and collect the corresponding CSI amplitude and phase difference data for each training moisture content level. Thus, the size of training data is 5000 packets for all 5 training moisture content levels. For online moisture estimation, DeepWMD collects CSI data from 200 packets for each test moisture level.

In order to improve wheat moisture detection accuracy, the input values should be limited in the range (0,1) for LSTM classification. Thus we choose a zero mean normalization approach (Z-score standardization) to normalize the CSI amplitudes and phase differences data. The normalized value  $Z_i$  is computed by

$$z_i = \frac{x_i - \mu}{\rho}, \quad (2)$$

where  $x_i$  represents the raw CSI data in the  $i$ th packet,  $\mu$  and  $\rho^2$  are the mean and variance of the original data set, respectively.

### C. Offline Training

For offline training, we design a deep LSTM network with two layers for multi-class wheat moisture detection using features of different humidity levels from CSI data. The offline training module consists of a deep LSTM network and a softmax classifier.

1) *Deep LSTM Network*: The LSTM network is considered as a type of recurrent neural network (RNN), which can effectively handle long-range dependency in the dataset [32], [33]. It also overcomes the issues of vanishing or exploding gradients found in traditional RNNs. The LSTM network can leverage temporal information of CSI data for multi-class wheat moisture detection, where the hidden LSTM units can map input CSI data to output label from five different wheat moisture levels. As shown in Fig. 6, we design a two-layer LSTM network to achieve a stronger CSI data learning representation, thus improving the classification accuracy.

Moreover, we leverage the LSTM network to implement a mapping from the normalized CSI data  $\mathbf{z} = (z_1, z_2, \dots, z_T)$  over different time slots from  $t = 1$  to  $T$ , to an output label

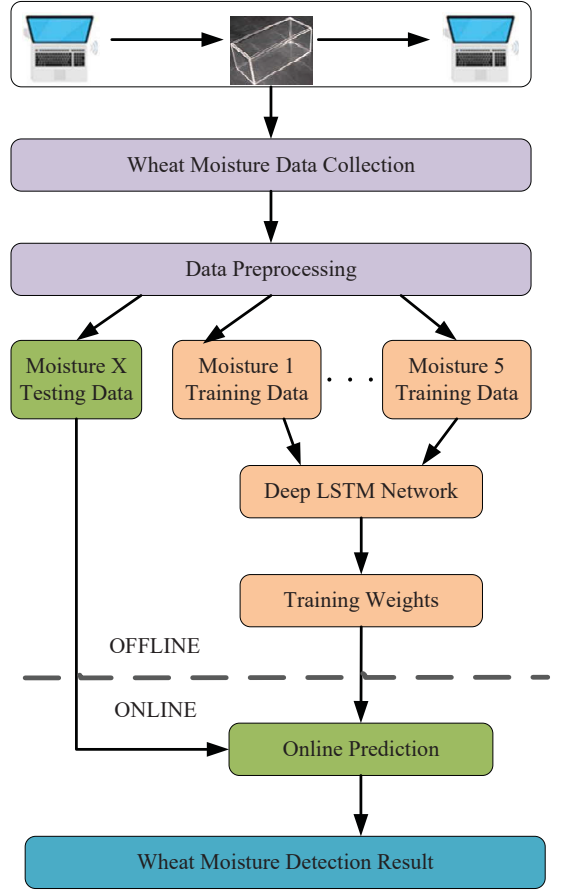


Fig. 5. The system architecture of DeepWMD.

$y$ , which is formulated by

$$i_t = \sigma(\omega_{ix}z_t + \omega_{im}h_{t-1} + b_i) \quad (3)$$

$$f_t = \sigma(\omega_{fx}z_t + \omega_{fm}h_{t-1} + b_f) \quad (4)$$

$$o_t = \sigma(\omega_{ox}z_t + \omega_{om}h_{t-1} + b_o) \quad (5)$$

$$g_t = \tanh(\omega_{cx}z_t + \omega_{cm}h_{t-1} + b_c) \quad (6)$$

$$c_t = f_t \odot c_{t-1} + i_t \odot g_t \quad (7)$$

$$h_t = o_t \odot \tanh(c_t), \quad (8)$$

where the  $\omega$  terms are the matrices of weights; the  $\mathbf{b}$  terms are the bias vectors;  $\tanh$  is the hyperbolic tangent function,  $\sigma$  is the sigmoid function;  $i$ ,  $f$ ,  $o$ ,  $g$  are the input gate, forget gate, output gate, candidate values, and cell activation, respectively;  $\mathbf{h}$  denotes the cell output activation vector; and  $\odot$  is the element-wise product of vectors. For the LSTM network, different gates control different data flows. For example, the input gate decides how much new data will be utilized in the current memory cell, and the forget gate decides how much data will be removed from the old memory cell. The output gate controls how much information will be output from the current memory cell. Using these gates, the LSTM network can effectively achieve multi-class wheat moisture detection

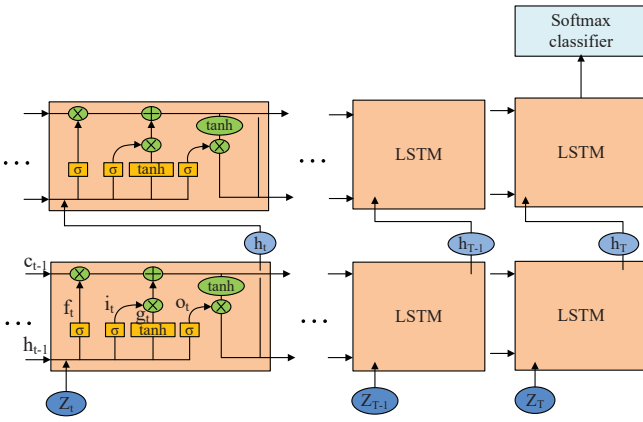


Fig. 6. The LSTM network architecture for offline training.

utilizing CSI data sequences.

2) *Softmax Classifier*: We use the softmax classifier to train the CSI data in the two layer LSTM network, where the output of the final cell's hidden node in the second layer is as the input of a fully connected layer. We denote the output of the softmax function as  $\mathbf{s} = [s_1, s_2, \dots, s_M]$ , which maps  $M$  input data vector to  $M$  normalized output data. We can formulate the softmax function by

$$s_i = \frac{e^{\mathbf{k}_f^T \boldsymbol{\omega}_i}}{\sum_{m=1}^M e^{\mathbf{k}_f^T \boldsymbol{\omega}_m}}, \quad i = 1, 2, \dots, M, \quad (9)$$

where  $\boldsymbol{\omega}_i$  is the weight vector of the fully connected layer,  $\mathbf{k}_f$  is the output vector of the final cell's hidden node in the second layer, and  $(\cdot)^T$  is the transpose operator.

For training LSTM weights, we denote  $L(\boldsymbol{\omega})$  be the loss function with the weight parameter  $\boldsymbol{\omega}$ . To measure the difference between the normalized output data and the true label data, a cross-entropy metric is employed. Moreover, we adopt  $L_2$  regularization hyperparameter to reduce the space of solutions, thus avoiding over-fitting. We formulate the loss function by

$$\max_{\boldsymbol{\omega}} L(\boldsymbol{\omega}) = - \sum_{i=1}^M y_i \log(s_i) + \frac{\eta}{2} \|\boldsymbol{\omega}\|_2^2, \quad (10)$$

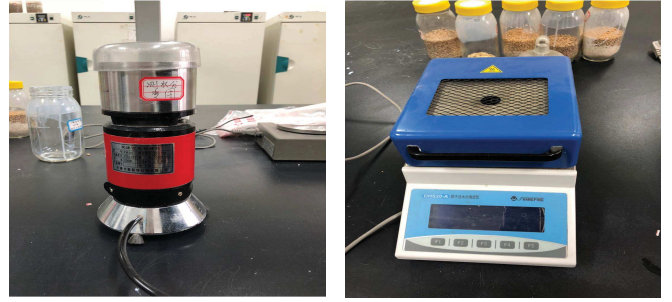
where  $y_i$  is the true labeled data for the  $i$ th wheat moisture level, and  $\eta$  is the hyperparameter for  $L_2$  regularization. Based on this loss function, we apply the Backpropagation Through Time (BPTT) algorithm to the LSTM network to train the parameters [32], where the Adam Optimizer is utilized to make LSTM network computationally efficient [42].

#### D. Online Forecast

After preprocessing  $N$  newly testing input data, we leverage the trained deep LSTM model with  $M$  training wheat moisture levels for online prediction. We define  $\boldsymbol{\beta}$  as the output results

TABLE I  
MOISTURE CONTENT CALIBRATION

Wheat sample	1	2	3	4	5
Moisture content	10.6%	11.3%	12.7%	14.1%	14.9%



(a) The high speed universal disintegrator. (b) The multi-function Infrared Moisture Analyzer.

Fig. 7. The oven-drying method.

of the Softmax classifier of the deep LSTM model, that is

$$\boldsymbol{\beta} = \begin{bmatrix} \beta_{11} & \beta_{12} & \cdots & \beta_{1N} \\ \beta_{21} & \beta_{22} & \cdots & \beta_{2N} \\ \vdots & \vdots & \ddots & \vdots \\ \beta_{M1} & \beta_{M2} & \cdots & \beta_{MN} \end{bmatrix}. \quad (11)$$

To reduce the variance of the output results, we need to obtain the average value of the  $N$  output results at every moisture level. We denote  $\beta_i$  as the average value of the output data vector  $[\beta_{i1}, \beta_{i2}, \dots, \beta_{iN}]$  in the  $i$ th row. Thus, we can obtain the mean vector as  $\bar{\boldsymbol{\beta}} = [\bar{\beta}_1, \bar{\beta}_2, \dots, \bar{\beta}_M]$ . Finally, the multi-class wheat moisture detection result  $D$  is obtained by

$$D = \operatorname{argmax}_{i \in \{1, 2, \dots, M\}} \bar{\beta}_i. \quad (12)$$

## IV. EXPERIMENTS AND EVALUATION

In this section, we first introduce the moisture content calibration operation, and then describe the prototype implementation of the DeepWMD system and the details of experimental settings. Finally, we evaluate the performance of DeepWMD with experiments.

### A. Moisture Level Calibration

We first calibrate the moisture content levels of five groups of wheat samples using the oven-drying method [8], where uses a high speed universal disintegrator and a multi-function infrared moisture analyzer as shown in Fig. 7. The moisture content levels are given in Table I for all the five wheat samples.

### B. DeepWMD Implementation

1) *Hardware and Software*: We leverage commodity laptops and Wi-Fi cards to implement the DeepWMD system. The prototype includes a Dell Latitude 5480 laptop with Intel(R)

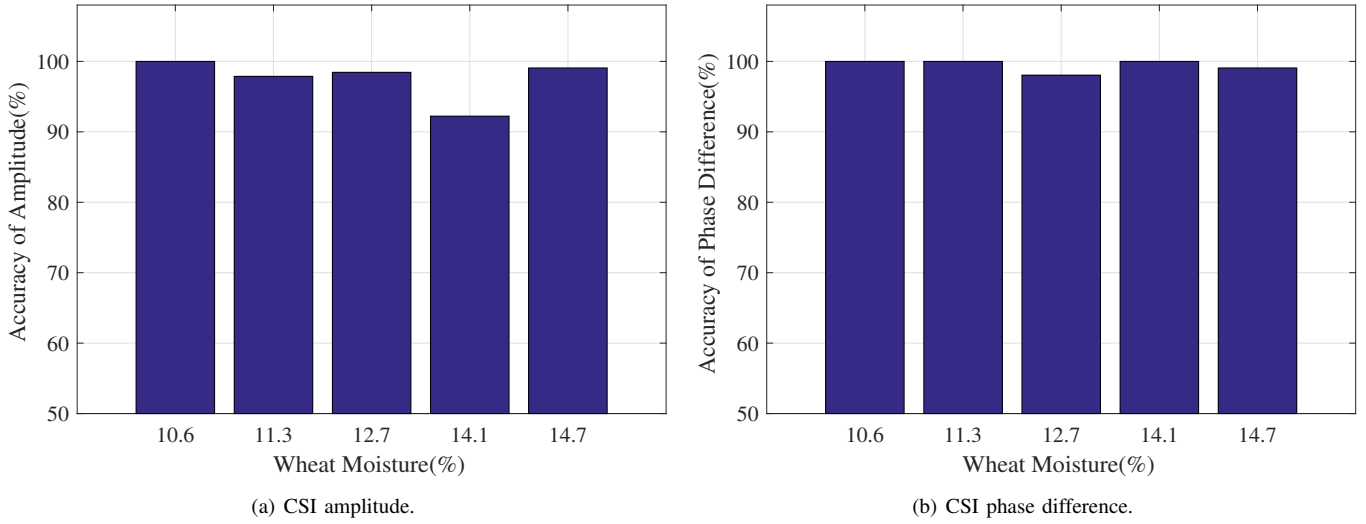


Fig. 9. Accuracy of multi-class wheat moisture detection for the LOS scenario.

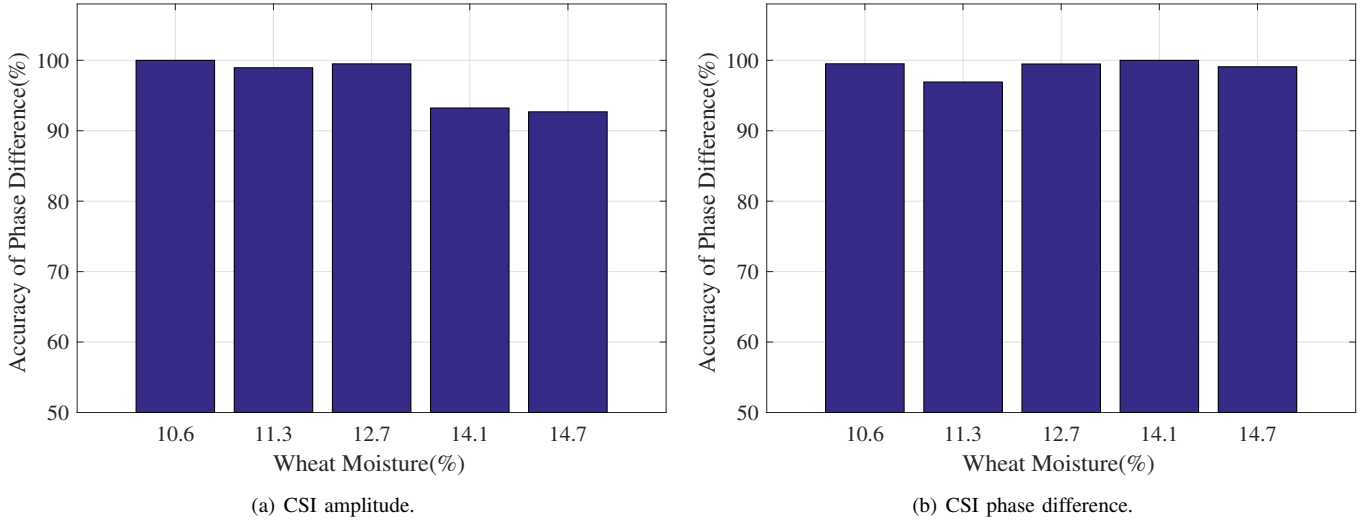


Fig. 10. Accuracy of multi-class wheat moisture detection for the NLOS scenario.



(a) The LOS experiment scenario. (b) The NLOS experiment scenario.

Fig. 8. Experimental setup for DeepWMD.

processor Pentium dual-core CPU as a receiver, and a Dell PP181 laptop as a transmitter, each installed with an Intel Link 5300 Wi-Fi NIC along with a modified device driver. Setting

the transmitter in the injection mode and the receiver in the monitor mode, we inject packets from the transmitter using one antenna to the receiver using three antennas, and collect CSI data for each received packet.

For the system software, the laptops run the 32-bit Ubuntu Linux14.04 operating system with kernel 4.1.10+. Then, we employ an LSTM model with two layers using Tensorflow to analyze CSI data and then implement multi-class wheat moisture detection [43].

2) *Experiment Scenario*: We conduct experiments to evaluate the performance of DeepWMD system in both LOS and NLOS scenarios in the research laboratory of Henan University of technology, Zhengzhou, P.R. China. We place the transmitter and the receiver at 3 m distance for both the LOS 8(a) and NLOS 8(b) scenarios. In the LOS case, the wheat is placed in the middle of the transmitter and the receiver. We send ICMP ping packets from the transmitter to

the receiver at 1000 packets/s.

### C. Performance Evaluation

We first evaluate the performance of DeepWMD in the LOS scenario. Fig. 9 shows the accuracy of multi-class wheat moisture detection for the LOS scenario using CSI amplitude (a) and phase difference data (b), respectively. Using CSI amplitude, we can notice that the DeepWMD can obtain the highest classification accuracy for wheat moisture detection, when the wheat moisture content level is 10.6%. For the wheat moisture content level of 14.1% the lowest classification accuracy for wheat moisture detection is 92.23%. Moreover, the average accuracy of five cases is about 97.53%. On the other hand, when CSI phase difference data is employed, the average accuracy of wheat moisture detection is about 99.42%, which is higher than CSI amplitude data. In addition, the classification accuracy even reaches to 100% in three cases, 10.6%, 11.3% and 14.1%, respectively. Thus, by using using CSI amplitude or phase difference data, the proposed DeepWMD method can obtain a high classification accuracy for LOS scenario based on the deep LSTM approach.

We then investigate the performance of the proposed DeepWMD system in the NLOS scenario. Fig. 10 show the accuracy of classification for the NLOS scenario using CSI amplitude (a) and phase difference data (b), respectively. We can notice that the classification accuracy is above 90% for all the wheat moisture content level using CSI amplitude. Moreover, the average detection accuracy is about 96.9%. On the other hand, the detection accuracy is above 95% for all the wheat moisture content level using CSI phase difference, and the average classification accuracy is about 99%, which demonstrates that CSI phase difference can obtain better performance than CSI amplitude, because CSI phase difference can well capture the change of wireless channel.

### D. Impact of System Parameters

For the impact of parameters on the performance of multi-class wheat moisture detection, we mainly focus on the ratio of training data over test data, the number of layers in LSTM network, and different antennas in LOS and NLOS scenarios.

Fig. 11 shows the average detection accuracy for different ratios of training data over test data in LOS scenario. As we can see, when we use 80% CSI amplitude or phase difference data for training, the best accuracies for CSI amplitude and phase difference are 97.5% and 99.4%, respectively. Moreover, using only 20% CSI data for training, we obtain that the average accuracies for CSI amplitude and phase difference are 95.0% and 93.9%, respectively, which are still acceptable results. On the other hand, Fig. 12 shows the average detection accuracy for different ratios of training data over test data in NLOS scenario. We can see that when the ratio is above 0.6, the average accuracy for CSI amplitude is above 96%. Moreover, when the ratio is above 0.4, the average accuracy for CSI amplitude is above 98.0%.

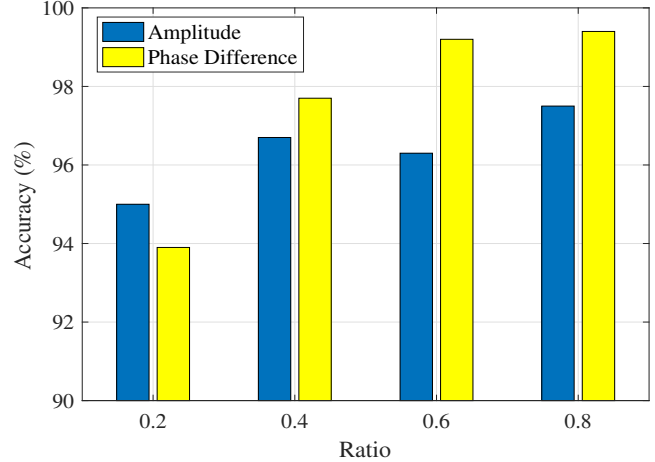


Fig. 11. Average detection accuracy for different ratios of training data over test data in LOS scenario.

Fig. 13 shows the average detection accuracy for different number of layers in LSTM network over test data in LOS scenario. As we can see, with the increase of the number of layers from 1 to 2, the average detection accuracy increases from 96.6% to 97.5% using CSI amplitude. When we employ CSI phase difference, the average accuracy increases from 99.1 % to 99.4%. On the other hand, Fig. 14 shows the average detection accuracy for different number of layers in LSTM network over test data in NLOS scenario. The multi-class detection accuracy for NLOS environment is decreased, comparing with for LOS environment. In fact, with the increase of the number of layers from 1 to 2, the average detection accuracy will increase from 96.2% to 96.8% and from 98.1% to 99.0% using CSI amplitude and phase difference data, respectively. Thus, increasing number of layers in LSTM network can obtain high multi-class detection performance for LOS and NLOS environments.

Fig. 15 shows the average detection accuracy for different antennas over test data in LOS scenario, where for phase difference, the antenna 1, 2, and 3 mean the antenna pair 1 and 2, the antenna pair 2 and 3, and the antenna pair 3 and 1, respectively. We can find that for different antennas or antenna pairs, the multi-class detection performance is almost same in LOS environment. Fig. 16 shows the average detection accuracy for different antennas over test data in NLOS scenario, where the phase difference has the same setting as Fig. 15. We can see that for CSI phase difference data, the highest detection accuracy is obtained by using antenna pair 1 and 2. We also find that for CSI amplitude data, the antenna 2 can achieve the best performance. In fact, the multi-class detection performance is almost same in NLOS environment. Thus, we only select the antenna 1 for the CSI amplitude method and antenna pair 1 and 2 for the CSI phase difference method in the above experiments.

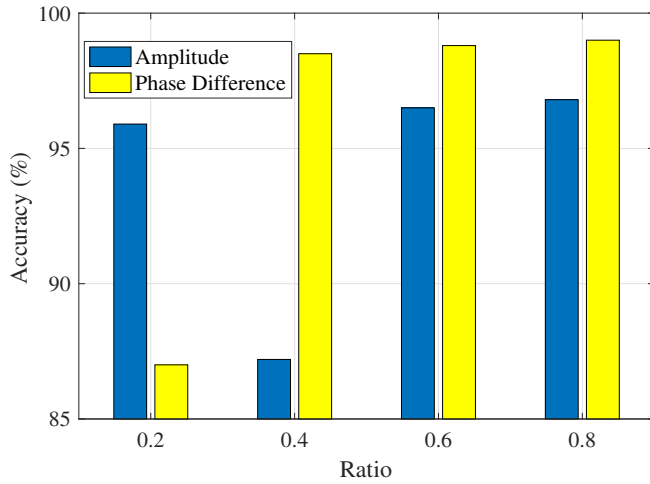


Fig. 12. Average detection accuracy for different ratios of training data over test data in NLOS scenario.

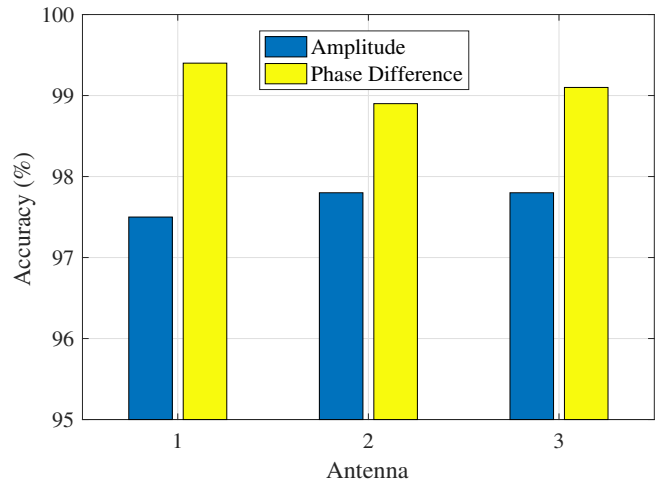


Fig. 15. Average detection accuracy for different antennas over test data in LOS scenario.

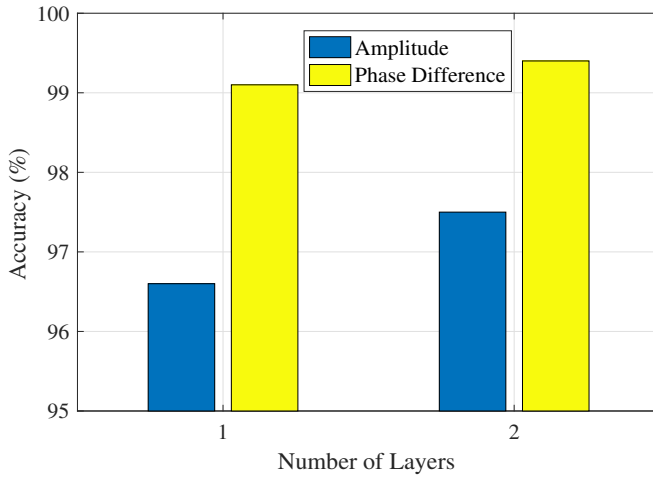


Fig. 13. Average detection accuracy for different number of layers in LSTM network over test data in LOS scenario.

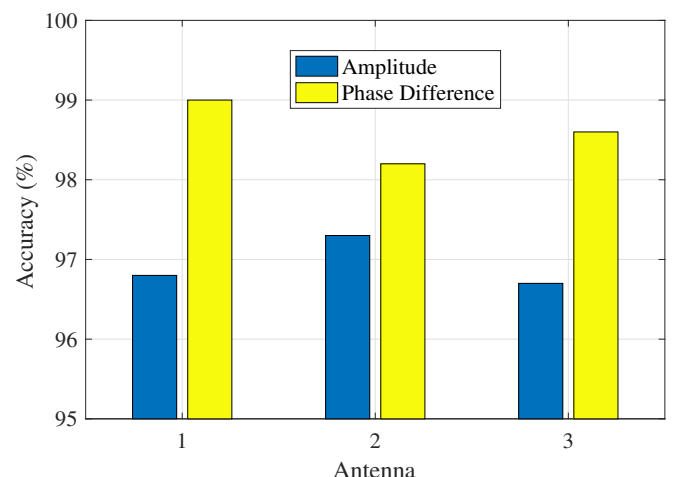


Fig. 16. Average detection accuracy for different antennas over test data in NLOS scenario.

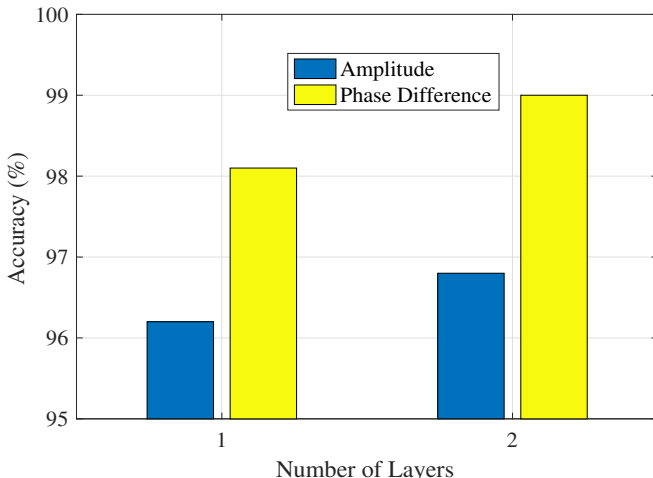


Fig. 14. Average detection accuracy for different number of layers in LSTM network over test data in NLOS scenario.

## V. CONCLUSIONS

In this paper, we proposed DeepWMD, a deep LSTM network based system for multi-class wheat moisture detection. The proposed system exploited CSI amplitude and phase difference data from commodity Wi-Fi devices for wheat moisture content detection. We designed and implemented the DeepWMD system with commodity Wi-Fi devices in the 5GHz band, which consisting of data preprocessing of collected CSI data, offline training, and online testing modules. Our experimental study demonstrated the efficacy of the proposed DeepWMD system, which was shown to achieve high-precision multi-class wheat moisture detection for both LOS and NLOS scenarios.

## ACKNOWLEDGMENT

This work is supported in part by the US NSF under Grant CNS-1702957, the Wireless Engineering Research and Education Center (WEREC) at Auburn University, Auburn,

AL, USA, and in part by the National Key Research and Development Program of China (2017YFD0401001) and by the NSFC (61741107).

## REFERENCES

- [1] D. Vasisht, et al., "FarmBeats: An IoT platform for data-driven agriculture," in *Proc. USENIX NSDI'17*, Boston, MA, Mar. 2017, pp. 515–529.
- [2] Z. Kapetanovic, D. Vasisht, J. Won, R. Chandra, and M. Kimball, "Experiences deploying an always-on farm network," *GetMobile: Mobile Computing and Communications*, vol. 21, no. 2, pp. 16–21, 2017.
- [3] H. M. Jawad, R. Nordin, S. K. Gharghan, A. M. Jawad, and M. Ismail, "Energy-efficient wireless sensor networks for precision agriculture: A review," *Sensors*, vol. 17, no. 8, p. 1781, 2017.
- [4] P. P. Jayaraman, A. Yavari, D. Georgakopoulos, A. Morshed, and A. Zaslavsky, "Internet of things platform for smart farming: Experiences and lessons learnt," *Sensors*, vol. 16, no. 11, p. 1884, 2016.
- [5] S. Wolfert, L. Ge, C. Verdouw, and M.-J. Bogaardt, "Big data in smart farming—a review," *Agricultural Systems*, vol. 153, pp. 69–80, 2017.
- [6] D. S. Jayas, "Storing grains for food security and sustainability," *Agricultural Research*, vol. 1, no. 1, pp. 21–24, Mar. 2012.
- [7] Y. Liu, W. Han, Y. Zhang, L. Li, J. Wang, and L. Zheng, "An internet-of-things solution for food safety and quality control: A pilot project in china," *Journal of Industrial Information Integration*, vol. 3, pp. 1–7, 2016.
- [8] American Society of Agricultural Engineers, "Moisture measurement—ground grain and seeds," pp. 567–568, Dec. 2001, ASAE Standard.
- [9] W. Wang and Y. Dai, "A grain moisture detecting system based on capacitive sensor," *International Journal of Digital Content Technology and its Applications*, vol. 5, no. 3, pp. 203–209, Mar. 2011.
- [10] Z. Liu, Z. Wu, Z. Zhang, W. Wu, and H. Li, "Research on online moisture detector in grain drying process based on v/f conversion," *Hindawi Mathematical Problems in Engineering Journal*, vol. 2015, p. Article ID 565764, 2015.
- [11] S. O. Nelson, A. W. Kraszewski, S. Trabelsi, and K. C. Lawrence, "Using cereal grain permittivity for sensing moisture content," *IEEE Trans. Instr. Meas.*, vol. 49, no. 3, pp. 470–475, June 2000.
- [12] K. Kim, J. Kim, C. Lee, S. Noh, and M. Kim, "Simple instrument for moisture measurement in grain by free-space microwave transmission," *Transactions of the ASABE*, vol. 49, no. 4, pp. 1089–1093, 2006.
- [13] Y. Yang, J. Wang, C. Wang, et al., "Study on on-line measurement of grain moisture content by neutron gauge," *Trans. Chinese Society of Agricultural Engineering*, vol. 16, no. 5, pp. 99–101, 2000.
- [14] D. Nath K, P. Ramanathan, and P. Ramanathan, "Non-destructive methods for the measurement of moisture contents—a review," *Sensor Review*, vol. 37, no. 1, pp. 71–77, Jan. 2017.
- [15] D. Halperin, W. J. Hu, A. Sheth, and D. Wetherall, "Predictable 802.11 packet delivery from wireless channel measurements," in *Proc. ACM SIGCOMM'10*. New Delhi, India: ACM, Sept. 2010, pp. 159–170.
- [16] X. Wang, L. Gao, S. Mao, and S. Pandey, "CSI-based fingerprinting for indoor localization: A deep learning approach," *IEEE Trans Veh Technol.*, vol. 66, no. 1, pp. 763–776, Jan. 2017.
- [17] —, "DeepFi: Deep learning for indoor fingerprinting using channel state information," in *Proc. WCNC'15*, New Orleans, LA, Mar. 2015, pp. 1666–1671.
- [18] X. Wang, L. Gao, and S. Mao, "BiLoc: Bi-modality deep learning for indoor localization with 5GHz commodity Wi-Fi," *IEEE Access Journal*, vol. 5, no. 1, pp. 4209–4220, Mar. 2017.
- [19] Y. Xie, Z. Li, and M. Li, "Precise power delay profiling with commodity wifi," in *Proceedings of the 21st Annual International Conference on Mobile Computing and Networking*. ACM, 2015, pp. 53–64.
- [20] J. Xiao, K. Wu, Y. Yi, and L. Ni, "FIFS: Fine-grained indoor fingerprinting system," in *Proc. ICCCN'12*, Munich, Germany, Aug. 2012, pp. 1–7.
- [21] X. Wang, L. Gao, and S. Mao, "Csi phase fingerprinting for indoor localization with a deep learning approach," *IEEE Internet of Things J.*, vol. 3, no. 6, pp. 1113–1123, Dec. 2016.
- [22] —, "PhaseFi: Phase fingerprinting for indoor localization with a deep learning approach," in *Proc. GLOBECOM'15*, San Diego, CA, Dec. 2015, pp. 1–6.
- [23] X. Wang, X. Wang, and S. Mao, "CiFi: Deep convolutional neural networks for indoor localization with 5GHz Wi-Fi," in *Proc. IEEE ICC'17*, Paris, France, May 2017, pp. 1–6.
- [24] —, "Resloc: Deep residual sharing learning for indoor localization with csi tensors," in *Proc. IEEE PIMRC 2017*, Montreal, Canada, Oct. 2017.
- [25] H. Wang, D. Zhang, Y. Wang, J. Ma, Y. Wang, and S. Li, "RT-Fall: A real-time and contactless fall detection system with commodity WiFi devices," *IEEE Trans. Mobile Comput.*, vol. 16, no. 2, pp. 511–526, Feb. 2017.
- [26] Y. Wang, K. Wu, and L. M. Ni, "Wifall: Device-free fall detection by wireless networks," *IEEE Trans. Mobile Comput.*, vol. 16, no. 2, pp. 581–594, Feb. 2017.
- [27] Y. Wang, J. Liu, Y. Chen, M. Gruteser, J. Yang, and H. Liu, "E-eyes: Device-free location-oriented activity identification using fine-grained wifi signatures," in *Proc. ACM Mobicom'14*, Maui, HI, Sept. 2014, pp. 617–628.
- [28] W. Wang, A. Liu, M. Shahzad, K. Ling, and S. Lu, "Understanding and modeling of WiFi signal based human activity recognition," in *Proc. ACM Mobicom'15*, Paris, France, Sept. 2015, pp. 65–76.
- [29] X. Wang, C. Yang, and S. Mao, "PhaseBeat: Exploiting CSI phase data for vital sign monitoring with commodity WiFi devices," in *Proc. IEEE ICDCS 2017*, Atlanta, GA, June 2017, pp. 1230–1239.
- [30] —, "Tensorbeat: Tensor decomposition for monitoring multi-person breathing beats with commodity WiFi," *ACM Transactions on Intelligent Systems and Technology*, vol. 9, no. 1, pp. 8:1–8:27, Sept. 2017.
- [31] W. Yang, X. Wang, A. Song, and S. Mao, "Wi-Wheat: Contact-free wheat moisture detection using commodity WiFi," in *Proc. IEEE ICC 2018*, Kansas City, MO, May 2018, pp. 1–6.
- [32] F. A. Gers, J. Schmidhuber, and F. Cummins, "Learning to forget: Continual prediction with LSTM," *Neural Computation*, vol. 12, no. 10, pp. 2451–2471, Oct. 1999.
- [33] K. Greff, R. K. Srivastava, J. Koutník, B. R. Steunebrink, and J. Schmidhuber, "LSTM: A search space odyssey," *IEEE Transactions on Neural Networks and Learning Systems*, vol. 28, no. 10, pp. 2222–2232, 2017.
- [34] A. Graves, N. Jaitly, and A.-r. Mohamed, "Hybrid speech recognition with deep bidirectional lstm," in *Proc. 2013 IEEE Workshop on Automatic Speech Recognition and Understanding (ASRU)*. IEEE, 2013, pp. 273–278.
- [35] F. J. Ordonez and D. Roggen, "Deep convolutional and lstm recurrent neural networks for multimodal wearable activity recognition," *MDPI Sensors*, p. 115, Jan. 2016.
- [36] X. Wang, Z. Yu, and S. Mao, "DeepML: Deep LSTM for indoor localization with smartphone magnetic and light sensors," in *Proc. IEEE ICC 2017*, Kansas City, MO, May 2018.
- [37] X. Wang, S. Mao, and M. X. Gong, "A survey of lte wi-fi coexistence in unlicensed bands," *GetMobile: Mobile Computing and Communications*, vol. 20, no. 3, pp. 17–23, 2017.
- [38] X. Wang, S. Mao, S. Pandey, and P. Agrawal, "CA2T: Cooperative antenna arrays technique for pinpoint indoor localization," in *Proc. MobiSPC 2014*. Niagara Falls, Canada: Elsevier, Aug. 2014, pp. 392–399.
- [39] Z. Yang, Z. Zhou, and Y. Liu, "From RSSI to CSI: Indoor localization via channel response," *ACM Comput. Sur.*, vol. 46, no. 2, p. 25, 2013.
- [40] X. Wang, C. Yang, and S. Mao, "ResBeat: Resilient breathing beats monitoring with online bimodal CSI data," in *Proc. IEEE GLOBECOM 2017*, Singapore, Dec. 2017.
- [41] C. Chen, Y. Han, Y. Chen, and K. R. Liu, "Indoor global positioning system with centimeter accuracy using wi-fi [applications corner]," *IEEE Signal Processing Magazine*, vol. 33, no. 6, pp. 128–134, 2016.
- [42] D. Kingma and J. Ba, "Adam: A method for stochastic optimization," *arXiv preprint arXiv:1412.6980*, 2014.
- [43] M. Abadi, A. Agarwal, P. Barham, E. Brevdo, Z. Chen, C. Citro, G. S. Corrado, A. Davis, J. Dean, M. Devin, et al., "Tensorflow: Large-scale machine learning on heterogeneous distributed systems," *arXiv preprint arXiv:1603.04467*, 2016.